



Visible light active photocatalyst: Hydrothermal green synthesized TiO₂ NPs for degradation of picric acid



D. Hariharan^a, A. Jegatha Christy^b, Jeyanthinath Mayandi^c, L.C. Nehru^{a,*}

^a Department of Medical Physics, School of Physics, Bharathidasan University, Tiruchirappalli, Tamilnadu, India

^b PG & Research Center of Physics, Jayaraj Annapackiam College for Women, Periyakulam, Tamilnadu, India

^c Department of Materials Science, Madurai Kamaraj University, Madurai, Tamilnadu, India

ARTICLE INFO

Article history:

Received 17 January 2018

Received in revised form 14 March 2018

Accepted 17 March 2018

Available online 19 March 2018

Keywords:

Green synthesis

Picric acid

Aloe Vera

Photocatalysis

ABSTRACT

Recent research on photocatalytic activities has been investigated using visible light region rather consuming ultraviolet region. In this Paper, a facile and eco-friendly method was developed to the synthesis of TiO₂ NPs using Aloe Vera gel (AV-TiO₂). The synthesized nanoparticles were characterized using XRD, XPS, HRTEM, EDAX and Raman spectroscopy. The sharp peaks by XRD pattern show the crystallinity and purity of titanium dioxide nanoparticles. The shape and morphology were studied by HR-TEM images and confirms the NPs size which falls in the range from 6 to 13 nm. Raman spectrum and XPS shows the energy modes and oxidation state of synthesized TiO₂ NPs. TiO₂-mediated photo-degradation of trinitrophenol (Picric acid- PA) irradiated by visible light source has also been investigated.

© 2018 Published by Elsevier B.V.

1. Introduction

The metal oxide nanoparticles play a very important role in the synthesis of materials, preserving the environment, production, and conservation of energy. Titanium dioxides (TiO₂) possess the strong medical applications among all the nanoparticles, because of its strong oxidation power, non-toxicity, and chemical stability [1]. TiO₂ has its applications in the areas of solar energy cells, environmental purification, electronic devices, gas sensors, photo-electrodes and photo-catalysts [2]. Titanium dioxide has emerged because of the properties like photo induced super-hydrophobicity and antifogging effect, hence it is helpful in the environmental purification by removing bacteria and harmful organic materials from water and air [3,4]. In the recent years, a number of physical and chemical methods were reported for the synthesis of nanostructures which are less eco-friendly and cost-effective. The chemical synthesis of nanoparticles produces a lot of toxic substances where the green synthesis of nanoparticles is easy, efficient, and eco-friendly. The biomolecules present in plants act as capping and reducing agents by stopping the agglomeration of nanostructures and promote their stability [5]. *Aloe barbandensis miller*, commonly known as aloe Vera is a very succulent plant species and had been used only as an herbal medicine in the past.

Tanaka K et al. [6], reported the photocatalytic degradation of picric acid using TiO₂ in the ultraviolet region. Umabala AM et al. [7], reported visible light active photocatalytic degradation of picric acid within 3 to 4 h using BiVo₄ + H₂O₂. Visible light active degradation of Methylene blue using green synthesized TiO₂ nanoparticles reported by Muniandy SS [8]. Also, Picric Acid (PA) is a strong irritant, allergen and environmentally pollutant [9]. In this paper, we have reported the synthesis of TiO₂ nanoparticles using Aloe Vera gel and studied the degradation efficiency of PA in the visible region. To our knowledge, it is the first report for explosive compound degradation in visible region using green synthesized TiO₂ nanoparticle.

2. Materials and methods

2.1. Hydrothermal synthesis of TiO₂ nanoparticles

Aloe Vera skin was peeled and the gel was washed seven times in the running water. 10 mL of Aloe Vera gel was added into 100 mL of deionized water and stirred for one hour. To this aqueous solution, 0.1 M of titanium (IV) isopropoxide was added drop by drop wise. The reaction mixture was stirred continuously for one hour at 20 °C. The solution was kept in an autoclave at 180 °C for 4 h. Then the prepared solution was heated on a hot plate at 80 °C. The obtained product was pounded finely and then calcinated in a muffle furnace at 500 °C for 5 h. Finally, Aloe Vera mediated TiO₂ nanoparticles (AV-TiO₂) was obtained.

* Corresponding author.

E-mail address: lcnehru@bdu.ac.in (L.C. Nehru).

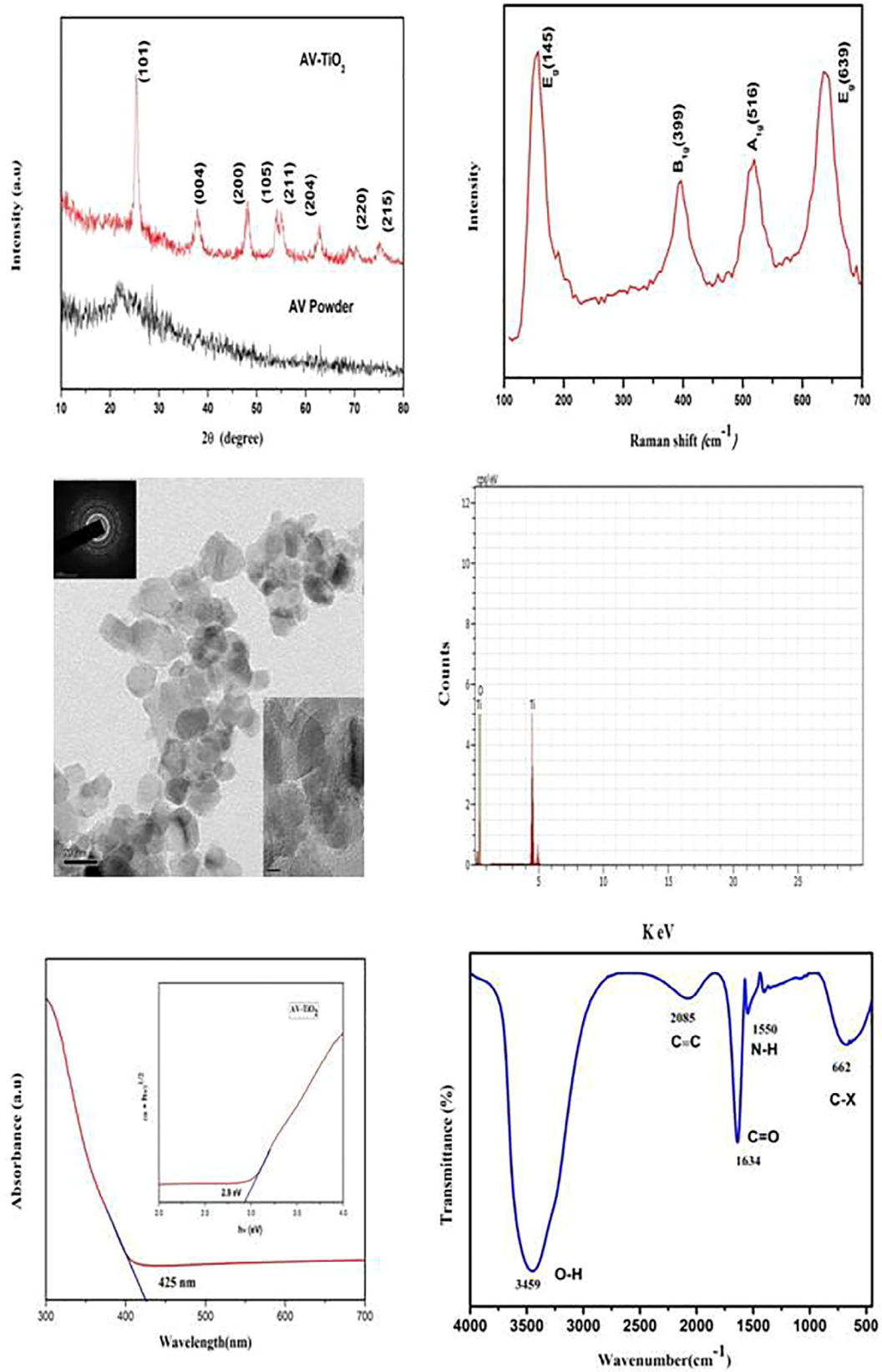


Fig. 1. (A) XRD spectra (B) Raman spectrum (C) HR-TEM image and (D) EDAX spectrum for the green synthesized AV-TiO₂. (E) UV-Vis spectrum for green synthesized TiO₂ NPs (F) FT-IR spectrum of 500 °C calcined Aloe Vera gel.

2.2. Characterization of TiO₂ nanoparticles

XRD analysis was performed using XPERT – PRO equipped with CuK α radiation. The structural property was also investigated using Raman spectroscopy, in the range of 100–700 cm⁻¹ using Renishaw equipment. High-Resolution Transmission Electron Microscopy (HRTEM) and Selected Area Electron Diffraction (SAED) images we obtained using JEM-2100F field emission TEM. Energy dispersive X-ray spectrometry (EDS) was performed with a spectroscope attached to TEM.

2.3. Photocatalytic experiments

Photocatalytic activities of the AV-TiO₂ were evaluated by the degradation of PA. In each experiment, 20 mg of TiO₂ catalyst was added in 100 mL of PA solution (500 mg/L) to obtain the catalyst at 200 mg/L. The experiments were carried out in a Pyrex beaker illuminated with a 15 W high-pressure mercury lamp emitting visible light (543 nm). The distance between the lamp and the pyrex beaker is about 12 cm. Prior to visible light irradiation, the suspension was stirred for 30 min in dark to reach the adsorption-desorption equilibrium. The solution was continuously stirred during the experiments. At given irradiation time intervals, 5 mL of the suspension was collected. The PA concentration was evaluated by UV–visible spectra monitoring the absorption maximum. A calibration plot based on Beer–Lambert's law was estab-

lished by relating the absorbance to the concentration. In each case, blank experiments were also conducted with the catalysts in the absence of light and without the catalysts when the solution containing the dissolved picric acid was illuminated. Moreover, Photocatalytic experiments were performed only under the visible region by using UV cut-off filter and in the same conditions with different milligram (10–50) of AV-TiO₂ catalyst were studied.

3. Results and discussion

The X-Ray diffraction patterns of the AV-TiO₂ are shown in the Fig. 1. The XRD pattern agrees with the JCPDS card No 89 – 4921 (anataseTiO₂). The XRD peaks 25.3°, 37.8°, 48.0°, 53.9°, 55.1°, 62.7°, 68.8°, 70.3° and 75.1° can be attributed to the respective 'hkl' planes of the crystalline structure of the AV-TiO₂. The crystalline size of the AV-TiO₂ can be calculated using the Scherer's formula and found to be 9 nm. In Fig. 1(A), no diffraction pattern absorbed for Aloe Vera powder, because of its amorphous nature.

The morphological information and particles size are determined using HR-TEM. Fig. 1(C) exhibits the tetragonal shape. The particle size range is 6 nm–13 nm with moderate variations in size. The Dotted rings in Selected Area Electron Diffraction are well matched to the XRD 'hkl' miller indices. The lattice springs is indicating AV-TiO₂ nanoparticles is crystalline in nature. In green synthesized TiO₂ nanoparticles, Ti percentage is 52 and O percentage is 48.

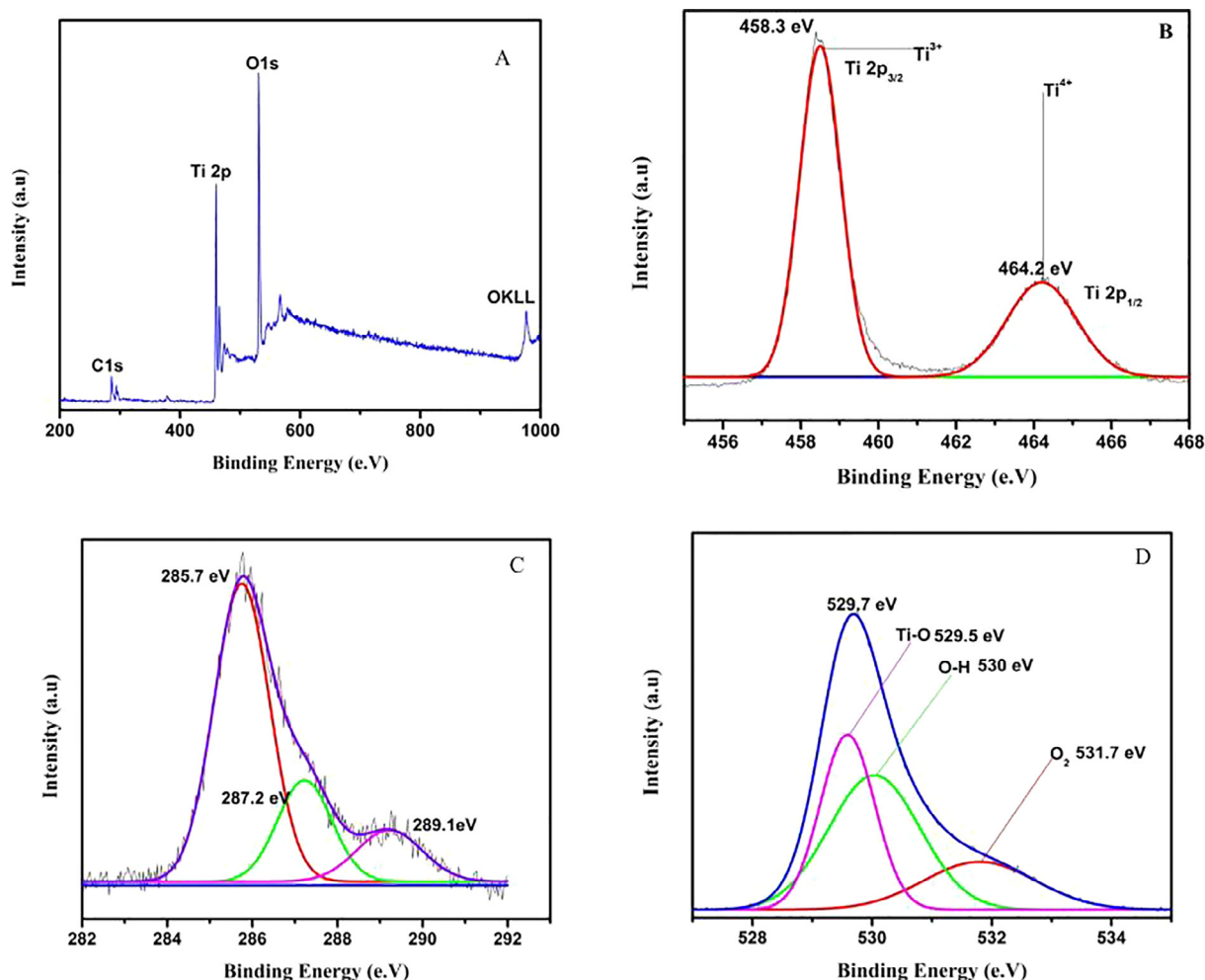


Fig. 2. XPS spectra of TiO₂ samples: (A) survey spectra of TiO₂; (B) Ti2p state; (C) C1s (D) O1s.

AV-TiO₂ absorption spectra (425 nm) shows a shift towards the visible region (Fig. 1E), so band gap energy (2.9 eV) is reduced compared to pure anatase TiO₂ (3.2 eV). This indicates the electron holes pairs are generated during visible light irradiation, which may contribute to the significant improvement in the photocatalytic activity in the visible light region. More importantly, the presence of Ti³⁺ sites with narrow band gap is identified by XPS, which is also a vital factor in improving the response of TiO₂ to the visible region.

Fig. 1F shows FTIR spectrum of Aloe Vera gel after calcination 500 °C in which the peaks at 3459 cm⁻¹ and 2085.8 cm⁻¹, in the spectra, are due to stretching of the O–H (Alcohol) and C≡C (Alkyne) group. The peaks corresponding to 1634 cm⁻¹, 1550 cm⁻¹, and 662 cm⁻¹ were indicated as the functional groups of C=O (carbonyl, stretching), N–H (amide, bending), and C–X (Halogen). The obtained products are the result of the organic compounds like are enzymes, vitamins, lignin's, monosaccharide, polysaccharides, salicylic acids, amino acids and sterols present in the leaf extract of Aloe Vera. It is well matched to XPS carbon spectra.

XPS explains about the elemental composition of AV-TiO₂. The survey spectra (Fig. 2A) show that the Ti, C, and O elements exist on the surface of the AV-TiO₂ sample. The TiO₂ sample was carbon

element can be ascribed to the adventitious carbon-based contaminant. Fig. 2B shows the peaks at 458.3 and 464.2 eV, which correspond to Ti 2p_{3/2} and Ti 2p_{1/2}, respectively. The peak position between Ti 2p_{3/2} and Ti 2p_{1/2} lines at 5.7 eV, suggest the existence of the Ti⁴⁺ oxidation state [10]. The peak at 464.2 eV, attributed to Ti⁴⁺ species, and the other centered on 458.3 eV corresponding to Ti³⁺ species [11]. Certainly, the presence of Ti³⁺ oxide with narrow band gap may be advantageous to the higher photocatalytic activity of the AV-TiO₂ nanostructures driven by visible light [12]. Fig. 2C C1s peak at 285.7 eV BE (major peak), which corresponds to the carbon atoms within the amino acids, vitamins, lignin, monosaccharide, anthraquinones, enzymes, minerals, salicylic acids, polysaccharides, saponins and sterols of Aloe Vera gel binding energy peaks at 287.2 and 289.1 eV were observed. The higher binding energy peak at 289.1 eV was attributed to electron emission from carbons in carbonyl groups [13]. (Carbonyl carbons of the polysaccharides or proteins-enzymes). The lower peak at 287.2 eV binding energy was most likely from carbons to the carbonyl carbons. XPS spectra of O1s in the AV-TiO₂ samples (Fig. 2d). The wide and asymmetric O1s spectra indicate that there would be three components, which can be further fitted into three peaks of oxygen (O_{Ti-O} at 529.5 eV), hydroxyl groups (O_{O-H} at 530 eV) [14], and adsorbed O₂ (at 531.7 eV) [15].

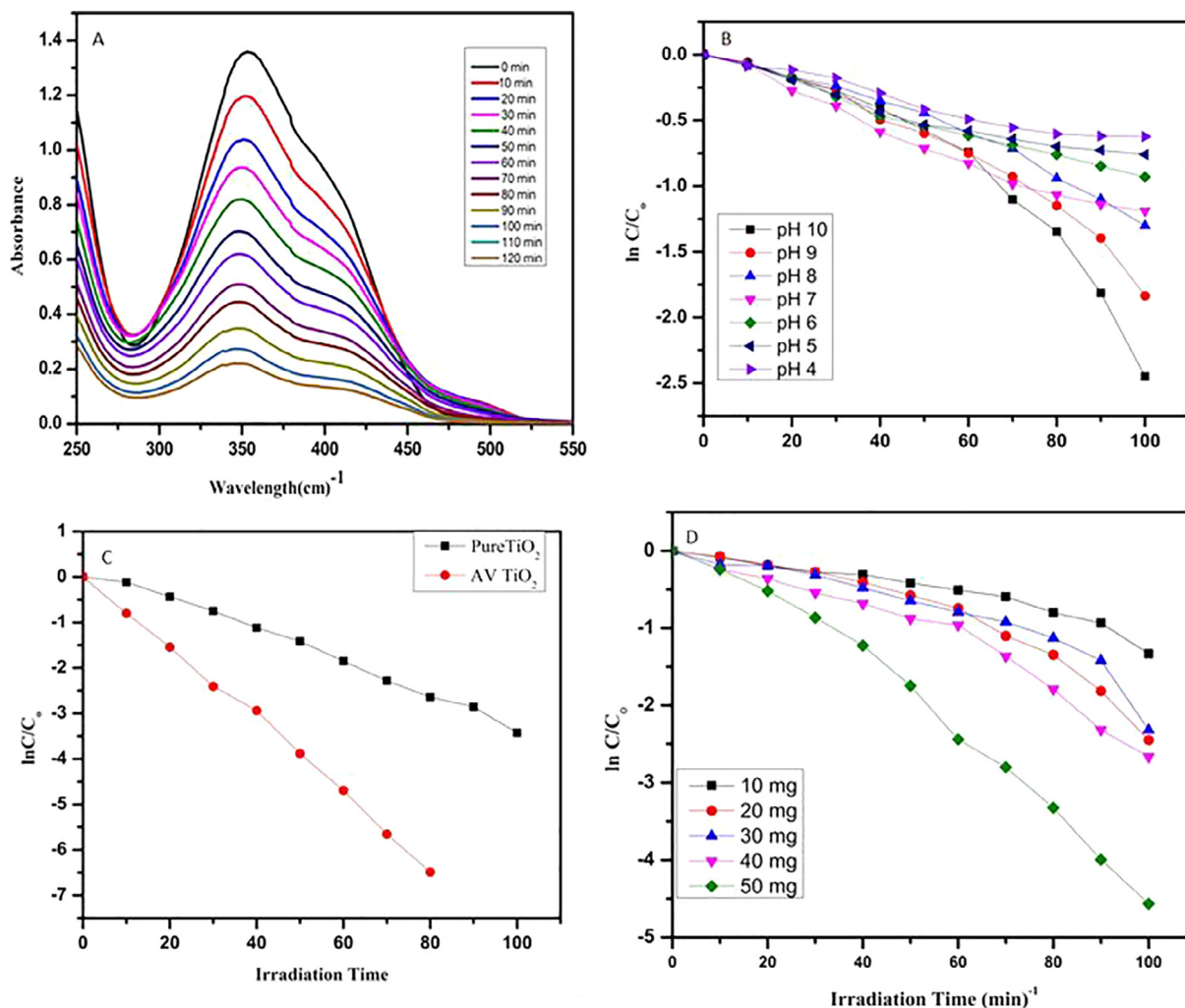


Fig. 3. (A) UV-Vis (DRS) absorption spectra for degradation of picric acid AV-TiO₂ kinetic linear simulation curves of PA photocatalytic degradation with (B) pH variation (C) Catalyst variation (D) Mg Variation.

3.1. Photocatalytic studies

From Fig. 3, as expected the AV-TiO₂ samples exhibit remarkable improvement in photocatalytic activity compared to that of the pure TiO₂. In Fig. 3a, 10 mg AV-TiO₂ catalyst treated PA absorbance spectra is observed in 0 min. After a time interval of each 10 min, the absorbance spectrum is decreased. The total absorbance spectrum of PA is decreased within 120 min. Fig. 3b explains, Acid is not degraded in acidic nature which is degraded in base condition, so pH value is increased, the Picric acid degradation rate is increased. In our experiment, PA is degraded in base condition (pH = 10). AV-TiO₂ concentration is increased, PA degradation rate is also increased (Fig. 3d), that indicates AV-TiO₂ concentration amount is increased, more free radicals are produced. The degradation order of photocatalytic activity for the samples can be summarized as follows: AV-TiO₂ > Pure TiO₂ (Fig. 3c).

The photocatalytic reaction can be considered as the process of generation, transfer, and consumption of the photo-generated carriers [16]. First, the photo catalyst absorbs the incident photons with energy above the semiconductor's band gap, generating electrons and the same amount holes. The holes abstract electrons from absorbed pollutants or react with H₂O to form hydroxyl radicals. However, the conduction band electrons reduce absorbed oxygen to form superoxide anions which can further disproportionate to form hydroxyl radicals via chain reactions. In addition, the electrons could react directly with the pollutant.

During visible light irradiation, the equilibrated Fermi level electrons were injected rapidly into the TiO₂ conduction band via a Surface Phonon Resonance (SPR) mechanism, and the injected electrons were trapped by dissolved oxygen molecules in water to yield high oxidative species, such as superoxide radical anions ([•]O₂⁻) and hydroxyl radicals (HO[•]) [17]. The TiO₂ facilitates electron-hole separation and subsequently helps in the formation of hydroxyl radicals. The superoxide radical anions ([•]O₂⁻) and hydroxyl radicals (HO[•]) produced under visible light irradiation might be responsible for mineralization of the organic pollutants [18]. The photocatalytic activity has a positive correlation with the formation rate of reactive radicals, i.e., faster formation radicals leading to a higher photocatalytic activity of the catalyst [19]. Overall, these results suggest that TiO₂ will help increase the rate of forma-

tion of [•]O₂⁻ and HO[•] reactive radicals due to AV-TiO₂ stimulate excess electrons ejection, and simultaneously facilitate the degradation of organic pollutants. The total amount of PA is degraded within 120 min when AV-TiO₂ is acting as a catalyst. As the concentration of AV-TiO₂ and pH level is increased, PA degradation is increased.

4. Conclusion

The AV-TiO₂ was synthesized successfully with Aloe Vera gel in a very simple and eco-friendly way. The physico-chemical properties of synthesized TiO₂ nanoparticles were investigated by XRD, XPS, HRTEM, EDAX and Raman spectroscopy analysis indicating that the synthesized TiO₂ nanoparticles are crystalline in the anatase phase with smaller size range and high surface area. AV-TiO₂ has enhanced photocatalytic activity for the degradation of picric acid in 120 min.

References

- [1] Kazuhito Hashimoto, Hiroshi Irie, Akira Fujishima, *Appl. Phys.* 44 (12R) (2005) 8269.
- [2] A. Karami, *Iran. Chem. Soc.* 7 (2) (2010) 154–S160.
- [3] Fujishima, Akira, and Kenichi Honda *nature*, 238, 5358, 1972, pp. 37–38.
- [4] Sachiko Tojo, *Phys. Chem. C* 112 (38) (2008) 14948–14954.
- [5] Makarov, V. V, *Acta Nat.* 6 1 (20) (2014).
- [6] Tanaka, Luesaiwong, Hisanaga *Mol. Cat. A Chem.* 18, 122, 1997, pp. 67–74.
- [7] A.M. Umabala, P. Suresh, A.P. Rao, *Der Pharma Chem.* 8 (6) (2016) 228–236.
- [8] Muniandy, Kaus, Jiang, Altarawneh, Lee, *RSC Adv.* 7, 76, 2017, pp. 48083–48094.
- [9] Gang He, *Mater. Chem.* 19 (39) (2009) 7347–7353.
- [10] Chen, Hua Wei, Young Ku, and Yu-Lin Kuo, *Chem. Eng. Technol.* 30, 9, 2007, pp. 1242–1247.
- [11] Chunyan Su, *CrystEngComm* 14 (11) (2012) 3989–3999.
- [12] Xiaoye Applied Xin, *Catal. B Environ.* 176 (2015) 354–362.
- [13] S. Li, Y. Shen, A. Xie, X. Yu, L. Qiu, Li Zhang, Q Zhang, *Green Chem.* 9 (2007) 852–858.
- [14] G.B. Hoflund, Z.F. Hazos, *Phys. Rev. B* 62 (2000) 11126–11133.
- [15] X.J. Quan, Q.H. Zhao, H.Q. Tan, X.M. Sang, F.P. Wang, Y. Dai, *Mater. Chem. Phys.* 114 (2009) 90–98.
- [16] Zhao, Jincai, Chuncheng Chen, and Wanhong Ma *Topics Catalysis*, 35, 3, 2005, pp. 269–278.
- [17] Liqiang Jing et al., *Chem. Soc. Rev.* 42 (2013) 249509–249549.
- [18] Peng Wang, *Phys. Chem. Chem. Phys.* 14 (28) (2012) 9813–9825.
- [19] Jing Liqiang, *Solar Energy Mater. Solar Cells* 90 (12) (2006) 1773–1787.